X-693-75-40

PREPRINT

NASA TM X- 70844

SCIENTIFIC INSTRUMENTATION OF THE RADIO-ASTRONOMY-EXPLORER-2 SATELLITE

N75-18284

(NASA-TM-X-70844) SCIENTIFIC INSTRUMENTATION OF THE RADIO-ASTRONOMY-EXPLORER-2 SATELLITE (NASA) 32 p HC $3.75 CSCL 22B G3/15 Unclas 13286

J. K. ALEXANDER
M. L. KAISER
J. C. NOVACO
F. R. GRENA
R. R. WEBER

FEBRUARY 1975

GSFC — GODDARD SPACE FLIGHT CENTER —
GREENBELT, MARYLAND

For information concerning availability
of this document contact:

Technical Information Division, Code 250
Goddard Space Flight Center
Greenbelt, Maryland 20771

(Telephone 301-982-4488)

"This paper presents the views of the author(s), and does not necessarily reflect the views of the Goddard Space Flight Center, or NASA."

SCIENTIFIC INSTRUMENTATION OF THE RADIO-ASTRONOMY-EXPLORER-2 SATELLITE

by

J.K. Alexander, M.L. Kaiser, J.C. Novaco
F.R. Grena and R.R. Weber
Radio Astronomy Branch
Laboratory for Extraterrestrial Physics
Goddard Space Flight Center
Greenbelt, Md. 20771

ABSTRACT

The RAE-2 spacecraft has been collecting radio astronomical measurements in the 25 kHz to 13 MHz frequency range from lunar orbit since June, 1973. This paper presents a summary of the technical aspects of the program including the calibration, instrumentation and operation of the RAE-2 experiments. Performance of the experiments over the first 18 months of the flight is summarized and illustrated. Among the unique features of the RAE-2 is the capability to observe repeated lunar occultations of strong radio sources at very low frequencies.

1. Introduction

The Radio Astronomy Explorer-2 satellite was placed into lunar orbit on 15 June, 1973, to provide radio astronomical measurements of the planets, the Sun, and the Milky Way over the frequency range of 25 kHz to 13.1 MHz. In this paper, we discuss the characteristics of the RAE-2 instrumentation in order to provide the background of technical details necessary for a full understanding of the scientific results obtained with the satellite data. Since RAE-2 is in many ways practically identical to RAE-1, we will concentrate on those areas where the two spacecraft are significantly different and refer the reader to an earlier discussion of the RAE-1 spacecraft (Weber et al., 1971) for further details and background on those items common to both satellites.

Among the major unexpected results from the four years of observations with the RAE-1 satellite (in Earth orbit) was the fact that radio emissions from the Earth - both natural and man-made - were very common and often very intense ($\geq$ 40 dB above the cosmic noise background) over the satellite's experiment frequency range of 0.2 to 9.2 MHz. Consequently, such a noisy environment often interferred with astronomical observations at low frequencies from Earth orbit. The second satellite in the RAE series was modified to be operated in lunar orbit where the terrestrial interference signals would be significantly weaker in

general and completely eliminated during occultation periods. In addition to those changes in systems required to place the spacecraft in the proper lunar orbit and return the data to the Earth, some improvements were made to the scientific experiments to take advantage of the wider frequency range afforded by the low interplanetary plasma density, to provide for observations with higher time resolution than RAE-1, and to implement other changes based on experience with the performance of the RAE-1 instruments.

2. General Description

Like RAE-1, the RAE-2 antenna systems are comprised of a pair of long, travelling-wave V-antennas deployed from opposite sides of the spacecraft body to form an X-configuration and a 37-m dipole which is extended along the minor symmetry axis of the system as shown in Fig. 1. Gravity gradient forces stabilize the spacecraft so that the upper V-antenna is always pointed away from the Moon to scan the celestial sphere and the lower V-antenna is always directed downwards toward the Moon. A fourth boom system - a 129-m libration damper - is deployed from an assembly suspended from below the main spacecraft body by means of a torsion wire. The libration damper boom is not utilized as an antenna but provides for damping of any spacecraft oscillations about

its equilibrium position by coupling spacecraft body energy of motion into the damper boom through both the torsion wire and a magnetic hysteresis system. The upper V-antenna is 229 m long and has an equivalent apex angle of 35°. Due to a mechanical flaw in one leg of the lower V-antenna which caused that leg to deploy nearly parallel to the local vertical, the lower V-antenna is asymmetrical in shape and was extended to a length of only 183 m during the first sixteen months of the flight before being deployed to 229 m in Nov. 1974. The asymmetry in the shape of the lower V-antenna results in a small angle between the spacecraft z-axis and the local vertical ($\sim 10^{\circ}$) and a similar offset of the direction of maximum gain of the lower V (Sayre, 1975).

RAE-2 is in a circular orbit having an altitude of 1100 km, an inclination of 59° to the lunar equator, and a period of 222 min. Fig. 2 shows two views of the celestial sphere as seen from the spacecraft in July of 1973 and 1974. The shaded areas are the regions occulted by the Moon during an orbit. Because of the upper-V/lower-V symmetry, the shaded areas also indicate the portion of the sky scanned with the upper-V during an orbit. These two views, separated by one year, illustrate how sky coverage is obtained through a combination of orbital scans and precession of the orbit plane at a rate of -0.14°/day

(retrograde) relative to the lunar equator. During the first year of operation, this translated into precession of -4.3 hr in right ascension and $+15^{\circ}$ in declination. Occultations of Jupiter began occurring once each orbit on July 26, 1973, and continued until July 10, 1974. Occultations of Saturn began June 1, 1974. Earth occultations occur for about seven days out of every 14 days and last up to 48 min each orbit. During these periods, data are recorded on the spacecraft tape recorder for playback when the satellite is in view on the lunar near side. An example of an occultation event will be shown in the last section of this paper.

For a period of two and one half months commencing every five months, RAE-2 experiences a solar eclipse of up to 48 min duration on every orbit. During these eclipse periods, the amount of sunlight available for battery charging is reduced, thus necessitating temporary shut-down of some or all of the experiments. Data coverage is as low as sixty percent during the minimum sunlight conditions.

For the first three weeks of RAE-2 operation beginning on 20 June, 1973, only the short, 37-m dipole antenna was deployed. During this period, the satellite was operated in a spin-stabilized mode (at 4 rpm) with the spin axis located in the ecliptic plane and normal to the spacecraft-Sun line. Spin modulation effects observed on solar radio

bursts during this phase of the mission provided the first information on the positions of low-frequency solar sources out of the ecliptic plane. Subsequently, the dipole booms were retracted, the spacecraft was reoriented, the long V-antennas and libration damper were extended, and the dipole was redeployed.

3. Antennas

Like their predecessors on RAE-1, the RAE-2 V-antenna booms are hollow, 1.3-cm diameter cylindrical tubes which are formed from heat-treated, silver-plated, beryllium-copper tape deployed in flight from motorized spools. Both the V-antenna booms and the dipole elements were designed with tabs along the edges of the tape which interlocked along the longitudinal seam in order to provide sufficient torsional rigidity to reduce boom motions resulting from varying solar illumination angles and thermal gradients. An insulating splice of Kapton was inserted between the V-antenna spool motor mechanism and the RF antenna terminal contacts at the base of the fully extended boom in order to reduce the shunt capacitance of the deployment mechanism to 70 pf (compared to 166 pf for RAE-1). Due to its smaller size and simpler design, the dipole boom deployment mechanism introduces a shunt capacitance at the antenna terminal of only 14 pf. A 600-ohm resistor is inserted 57m from the tip of each leg of the V-antenna booms. Hence, at frequencies at which the end section

beyond the terminating resistor is an odd number of quarter wavelengths (1.31, 3.93, 6.55, 9.18 MHz) the antenna has a travelling-wave current distribution between the root and the load resistor, and the back lobes of the antenna radiation pattern are suppressed by more than 10 dB.

The electrical properties of the travelling-wave V-antenna derived from theoretical studies, scale model measurements, and in-flight measurements in support of the RAE-1 mission are summarized by Weber et al. (1971) and by Alexander and Novaco (1974). The scale-model and in-flight measurements have served to provide general insight into the behavior of the travelling-wave V-antenna and to provide confirmation of the more versatile and detailed analytical calculations. The most detailed analytical studies of the radiation properties of the RAE-2 antennas have been performed by Sayre (1975). Using information on the actual in-orbit shapes of the booms, he calculated radiation patterns and impedances by employing the matrix method of moments described by Harrington (1967) and Harrington and Mautz (1967). In this approach, matrix methods are used to calculate the current distribution on the antenna by treating the spacecraft booms as an array of filamentary, elemental scatterers. A summary of the principal features of the calculated V-antenna radiation patterns over the RAE-2 frequency range is given in Table 1. The solid

angle of the main lobe varies from the order of a steradian above a few MHz, to approximately a hemisphere near 1 MHz, to nearly isotropic at the lowest frequencies where the antenna is short compared with a wavelength.

The upper V-antenna makes a series of scans across the Earth every 14 days, and we can derive an estimate of the gross behavior of the actual antenna properties by using the Earth as a calibration source. In Fig. 3 we have plotted relative occurrence of strong terrestrial signals at 6.55 MHz as a function of angular distance from the point of closest approach of the Earth to the local vertical for antenna lengths of 183 and 229 m. Due to the sporadic nature of the terrestrial emission and to the fact that the measurements were compiled using 4-day spans of data corresponding to about 50° of motion of the Earth with respect to RAE-2, the apparent main beam pattern tends to be broadened. The large E-plane first side lobes also probably contribute to a broader effective 6.55 MHz main beam for the 229-m antenna as compared with the 183-m antenna. (This difference is not obvious in the essentially identical great circle scans of the Galactic background compiled with the two antenna lengths.)

Theoretical analyses of the RAE-2 dipole antenna impedance (Sayre, 1975) show that the dipole radiation resistance is changed by interactions with the long V-antennas and libration

damper boom. The dipole radiation resistance is increased below 1 MHz and decreased above 1 MHz due to these interactions, and corrections for this effect were applied to RAE-1 data by Weber (1972). Since the dipole was the first antenna extended on RAE-2, it has been possible to compare the changes in the dipole performance resulting from extension of the other booms by looking at apparent changes in the Galactic background radiation. Increased radiation resistance will result in correspondingly increased noise levels at the receiver input. The RAE-2 data are in qualitative agreement with the expected effects. When the long booms were extended the dipole background levels increased at low frequencies and decreased at higher frequencies, confirming the predicted behavior.

4. Receivers

The receiving and calibration systems on RAE-2 are shown in the simplified block diagram in Fig. 4. A Ryle-Vonberg radiometer is connected to each V-antenna through a balun transformer. These radiometers are nine-channel, stepped-frequency devices which cover the range from 0.45 to 9.18 MHz and are essentially identical to those used on RAE-1. Although they normally make one frequency scan every 144 sec, they can also be operated in a fixed-frequency mode by ground command. Burst receivers are connected to all three antennas

by means of high input impedance, broad-band pre-amplifiers. The burst receivers are rapid sampling, stepped-frequency, total-power receivers and will be described in more detail below. They are calibrated in flight once every 20 min by a noise source whose signal can be injected into the burst receiver pre-amps either in place of the antenna signal or in addition to the antenna signal through an isolation resistor. Also every 20 min the upper V-antenna is connected to an impedance probe like that used on RAE-1 which measures the voltage, current and phase of a test signal at nine frequencies between 0.24 and 7.86 MHz.

The burst receiver pre-amplifiers have a gain-versus-frequency response which rolls off at high frequencies (~25 dB per octave, down 10 dB at 20 MHz) thereby providing some protection from interference effects due to intense out-of-band signals. However, because they operate over a very broad bandwidth, there are occasions when strong in-band signals can cause saturation and intermodulation problems which affect the performance at receiver channels other than at the received frequencies. Measurements have shown that such effects first become significant when the interfering signal levels are 50-60 dB above receiver threshold. The Ryle-Vonberg receivers have separate relatively narrow-band (200 kHz) pre-amplifiers for each frequency channel and are

less sensitive to this type of problem (80-90 dB selectivity). As a consequence, comparison of the data from the two types of receivers provides a check on the extent of non-linear effects in the burst receivers during intense noise events.

A simplified block diagram of the RAE-2 burst receiver is shown in Fig. 5. A balun transformer splits the RF signal between two identical back-ends consisting of a mixer, IF strip, and detector. Only one of the IF strips is powered at a given time; the other serves as a back-up system. A 16-crystal local oscillator is located in each half of the burst receiver, and the mixer outputs are shared by each IF strip so that the receiver covers 32 independent channels between 0.025 and 13.1 MHz. The IF crystal filter bandwidths are 20 kHz. Post-detection integration time constants are 6 ms in all burst receivers. Each mixer is preceded by low-pass filters which roll off steeply above 13 MHz in order to supress high-frequency signals near the intermediate frequency of 21.4 MHz. In the normal operating mode, one frequency scan is made every 4 sec on the dipole and every 8 sec on the V-antennas. The scan rate can be increased upon command by operating only the burst radiometer on the upper V-antenna or the dipole and obtaining a full frequency scan every 2 sec. Each burst receiver can also be commanded to operate in a fixed-frequency mode.

Procedures for calibrating the RAE-2 receivers prior to launch were very similar to those described by Weber et al. (1971) for RAE-1. Final calibration of the dynamic response of all receivers was performed after their integration onto the flight spacecraft by injecting broadband noise from a standard noise source through a variable precision attenuator and a dummy antenna network into the flight receivers. Such calibrations (which were conducted at -10, 6, 16, 26, and 35°C) were performed under computer control, and the spacecraft telemetry data were recorded directly on magnetic tape for computer processing. Sample calibration curves for the upper V-antenna receivers at 2.2 MHz are shown in Fig. 6. Each receiver has a total dynamic range of 60 dB which is divided into three 20-dB ranges for the Ryle-Vonberg radiometer and two 30-dB ranges for the burst receiver.

In-flight receiver performance has been very good to date. When background levels observed with the Ryle-Vonberg receivers during quiet times are averaged for four days (26 orbits), the standard deviation for the antenna temperature measurements of a given point in the sky is typically $\sim$ 5 percent. This is in agreement with the predicted fluctuation level derived from the cumulative effects of receiver noise, telemetry digitization step size, and calibration uncertainties. Gain changes in the Ryle-Vonberg receivers, deduced from measurements

of the average background level over each orbit during the first year of the flight, did not exceed 10%. As a consequence of this and the fact that the RAE-2 orbit precesses very slowly, it has been possible to average data accummulated over several months to provide great circle scans of the background brightness distribution with an internal consistency of $\sim$ 3 %. During the first twelve months the burst receivers on the V-antennas experienced a 38°C range of ambient temperatures. In-flight calibration levels during this period showed a total gain change of only $\sim$ 1 dB. After correction for known temperature effects, the burst receiver data indicate that residual gain variations did not exceed $\sim$ 10 % during the first year of the flight. A malfunction in control logic circuitry in the dipole burst receiver has resulted in unreliable data when the receiver temperature is above about 15°C. Consequently, there has been a significant loss in observations (about 60 %) from the dipole antenna.

5. Observations

The RAE-2 observations obtained from lunar orbit differ in character from the RAE-1 data in two important ways. At the lunar distance, RAE-2 is well separated from the emission regions of the Earth's magnetosphere and, thus, the Earth appears as an astronomical object in its own right. This

can impose periodicities of 29.5 days (the lunar synodic month) and 24.8 hours (the interval between consecutive sweeps of a given geographic position past the Moon) on the data at frequencies where the Earth is an active radio source. These striking noise enhancements are evident in Fig. 7 which displays the minimum antenna temperatures at selected frequencies recorded by the upper-V burst receiver during the last four months of 1973. Large increases in antenna temperature are seen at both high and low frequencies near each full Moon. Such enhancements were also observed by Grigoréva and Slysh (1970) with the Luna-11 and Luna-12 spacecraft. At 3.93 MHz, this is the time of maximum penetration of both man-made and thunder-storm radio noise (Herman and Stone, 1974) through the relatively transparent nighttime ionosphere. At the lower frequencies, radio emission caused by precipitating electrons in the auroral zones is at peak intensity at approximately 20-22 hr geomagnetic local time on Earth (Gurnett, 1974). RAE-2 is essentially "above" this region just prior to full Moon. A similar, but much less intense type of auroral zone radio emission occurs near local noon or new Moon (Kaiser and Stone, 1975). The 24.8-hr periodicity, most evident at 3.93 MHz, corresponds to passages of particular geographic coordinates past the sub-lunar-point; whereas at the low frequencies,

the auroral noise is related to the position of the geomagnetic pole as well as to local time.

Both the long-term stability of the receiving system and the available data coverage are also illustrated in Fig. 7. The slight change in level, particularly evident at 3.93 MHz in mid-November, results from the final V-antenna extension from 183 to 229 m.

The other, and perhaps more dramatic, difference between the RAE-2 and RAE-1 observations is the occurrence of lunar occultations of radio sources. As seen from the spacecraft, the Moon is a 76° diameter disk with a well defined edge. (The Earth as seen from RAE-1 had the same diameter but the "edges" of the Earth were not sharply defined or predictable because of gradients and inhomogeneities in the terrestrial ionosphere.) Source locations can be determined to a precision limited only by the uncertainty in calculation of the position of the lunar limb from ephemeris data. For worst case satellite ephemeris errors of ± 10 sec the resultant position uncertainty is ± 15 arc min. Fig. 2 shows the regions of the sky occulted at various times and the positions of some of the most intense discrete sources seen by ground-based radio telescopes. These sources form a starting list of possible candidates for occultation events. However, the most impressive occultations are those of the Earth. The terrestrial noise

sources referred to in Fig. 7 are seen on a much expanded time scale centered on an occultation of the visible Earth in Fig. 8. The top panel is a computer-generated dynamic spectral display of all 32 upper-V burst receiver channels with increasing intensity represented by increasing darkness. The auroral noise is the dark band running across the middle of the strip between 185 and 600 kHz. The lower panels show intensity-vs-time plots for several individual channels for the same period of time. The fact that the auroral noise does not disappear and reappear exactly coincident with the times of occultation of the visible Earth is evidence for the extended size of the source region. At the higher frequencies, however, the occultation of the thunderstorm and/or man-made noise occurs at the same time as the predicted geometrical occultation of the visible disk, confirming that this type of noise is generated at or near the Earth's surface.

The intense sporadic noise seen at the lowest few observing frequencies (below 100 kHz) in the dynamic spectrum is not diminished during Earth occultation, indicating a non-terrestrial origin. Grigoŕéva and Slysh (1970) observed diminutions of the high noise levels at 200 and 965 kHz when Luna-11 and Luna-12 where in lunar shadow, and they attributed this effect to shot noise generated by interaction of their 2.5-m antenna with the solar wind. Occasionally we also observe occultations of the very low frequency noise during solar eclipse;

however we do not see any evidence for continuously enhanced noise levels above 100 kHz. This result is not incompatible with the findings from the Luna experiments since the much longer RAE-2 antennas are much less susceptible to shot noise effects.

In addition to the Earth, occultations of the Sun (Fainberg, 1975) and Jupiter have been detected. The potential occultation candidates of Fig. 2 are much less intense radio sources and, thus, require rather sophisticated averaging techniques for detection which are currently being developed.

Major observing programs with the RAE-2 are being conducted in the areas of Galactic astronomy, solar astronomy, and planetary astronomy. Observations of the Galactic background distribution with the 229-m upper V-antenna will supplement earlier RAE-1 measurements by providing wider frequency coverage ($\sim$ 1 to 10 MHz) and new data at declinations above 60^{o}. New information on the locations of solar radio sources between <10 and 200 $R_{\odot}$ is becoming available from measurements of lunar occultations of solar bursts. Enormous detail regarding the Earth as a low-frequency radio source is now available from the perspective of the lunar orbit. A comprehensive search for other radio sources including the planets, Galactic objects, and extragalactic sources is now under way, and with the eternal optimism shared by all astronomers we can look for the greatest surprises to come from unpredicted results of that search.

Acknowledgements

A project as large and complex as RAE-2 depends on the efforts of many individuals for its success. We especially want to acknowledge the contributions of Project Manager J.T. Shea, Project Scientist R.G. Stone, our colleagues in the Radio Astronomy Branch who collaborated in all phases of the RAE-2 experiments and the talented engineers and technicians at Goddard who built the RAE-2 spacecraft and guided it into lunar orbit in good health.

Table 1. Summary of the radiation characteristics of the 229-m V-antenna

Freq.	θ_E(FWHM)	θ_H(FWHM)	1st Side Lobe	Front:Back
9.18 MHz	37°	61°	-2 dB	~10 dB
6.55	27	55	-4	~15
3.93	80	63	-5	~15
1.31	180	120	-12	~15
0.87	220	160	--	~15

References

Alexander, J.K., and Novaco, J.C. 1974 Astron. J. 79, 777.

Fainberg, J. 1975 in press.

Grigoťeva, V.P., and Slysh, V.I. 1970 Kosmich. Issled. 8, 284.

Gurnett, D.A. 1974 J. Geophys. Res. 79, 4227.

Harrington, R.F., and Mautz, J.R. 1967 IEEE Trans. Ant. Prop. AP-15, 502.

Herman, J.R., and Stone, R.G. 1974 Meeting of U.S. National Committee of URSI, Boulder, Colorado.

Kaiser, M.L., and Stone, R.G. 1975 Science, in press.

Sayre, E.P. 1975 in press.

Weber, R.R., Alexander, J.K., and Stone, R.G. 1971 Radio Science 6, 487.

Figure Captions

FIG. 1 - Diagram of the RAE-2 boom configuration during the first sixteen months of operation. The lower V-antenna booms were extended to their full 229-m length in November, 1974.

FIG. 2 - Projection of the RAE-2 orbit in celestial coordinates showing that portion of the sky occulted by the Moon during the first year of the mission.

FIG. 3 - Estimate of the size of the upper V-antenna main beam at 6.55 MHz derived from scans of the Earth.

FIG. 4 - Block diagram of the RAE-2 experiment instrumentation.

FIG. 5 - Block diagram of the RAE-2 burst receiver.

FIG. 6 - Sample calibration curves for the Ryle-Vonberg radiometer and burst receiver on the upper V-antenna for three different ambient temperatures.

FIG. 7 - Plot of the minimum signal level for each ten-minute interval observed at selected frequencies with the upper V-antenna during August through December, 1973.

FIG. 8 - Example of a lunar occultation of the Earth as observed with the upper-V burst receiver. The top frame is a computer-generated dynamic spectrum; the other plots display intensity vs. time variations at frequencies where terrestrial noise levels are

PRECEDING PAGE BLANK NOT FILMED

often observed. The 80-sec data gaps which occur every 20 min are at times when in-flight calibrations occur. The short noise pulses observed every 144 sec at the highest frequencies during the occultation period are due to weak interference from the Ryle-Vonberg receiver local oscillator on occasions when both that receiver and the burst receiver are tuned to the same frequency.

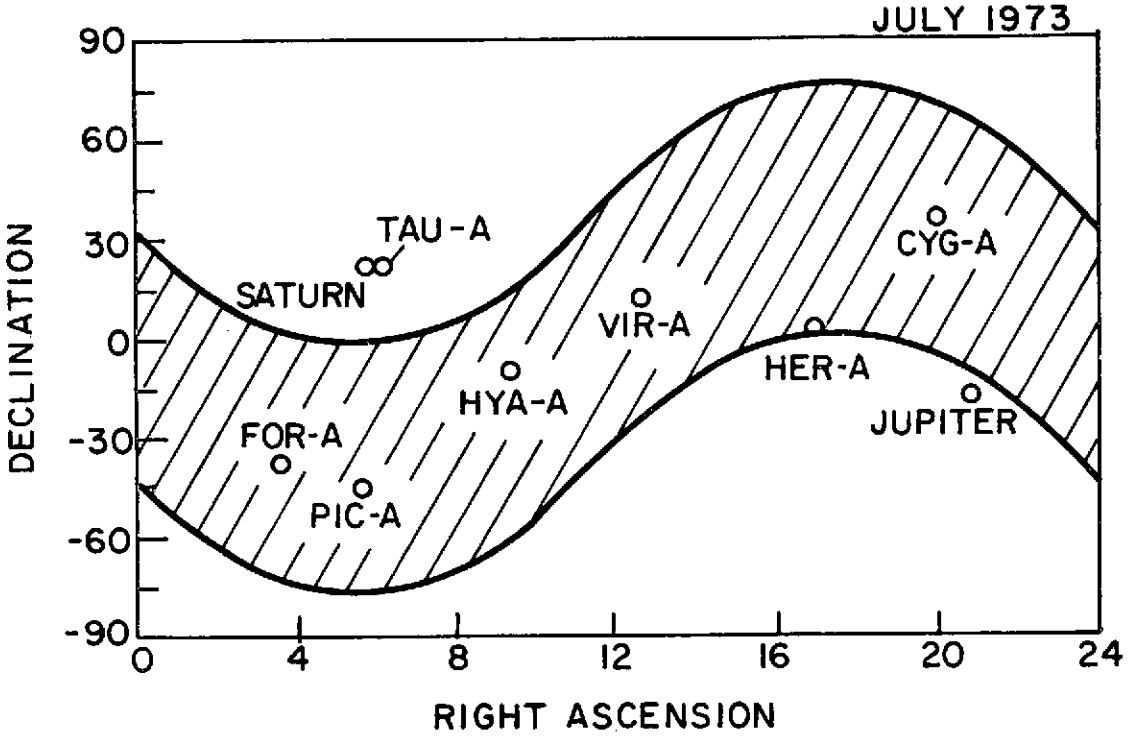
JULY 1973
90
60
30
0
-30
-60
-90
DECLINATION
TAU-A
SATURN
VIR-A
CYG-A
HER-A
HYA-A
JUPITER
FOR-A
PIC-A
0
4
8
12
16
20
24
RIGHT ASCENSION

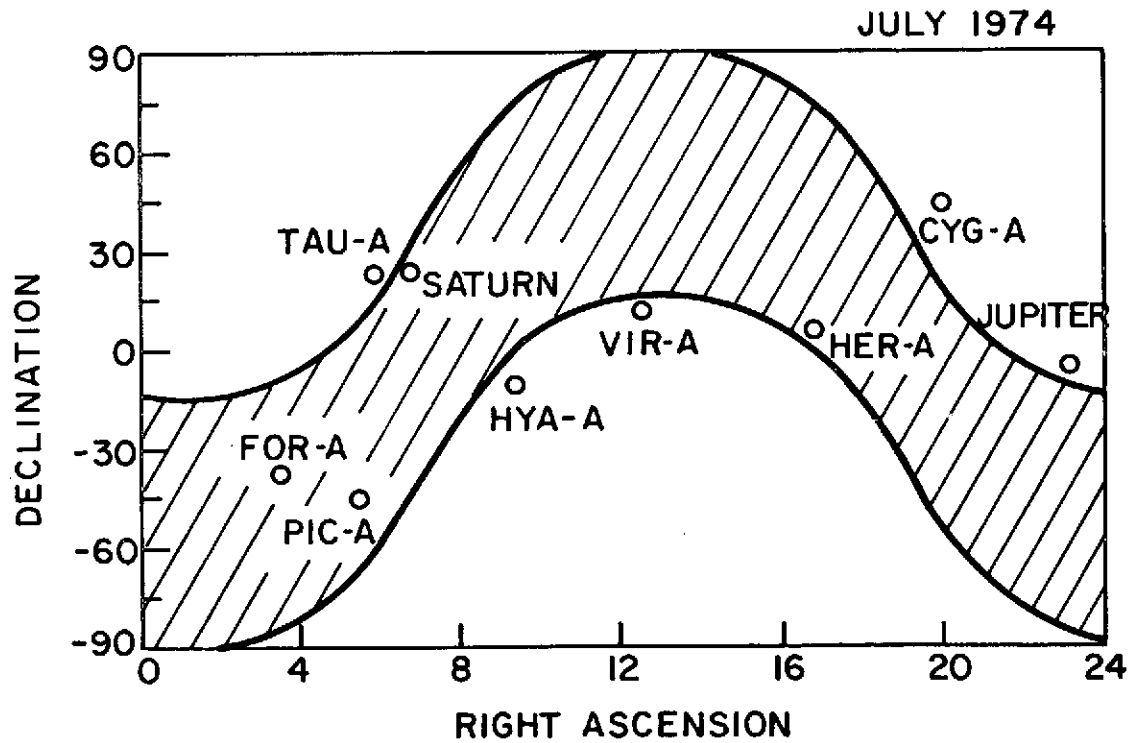
JULY 1974
90
60
30
0
-30
-60
-90
DECLINATION
TAU-A
SATURN
CYG-A
JUPITER
VIR-A
HER-A
HYA-A
FOR-A
PIC-A
0
4
8
12
16
20
24
RIGHT ASCENSION

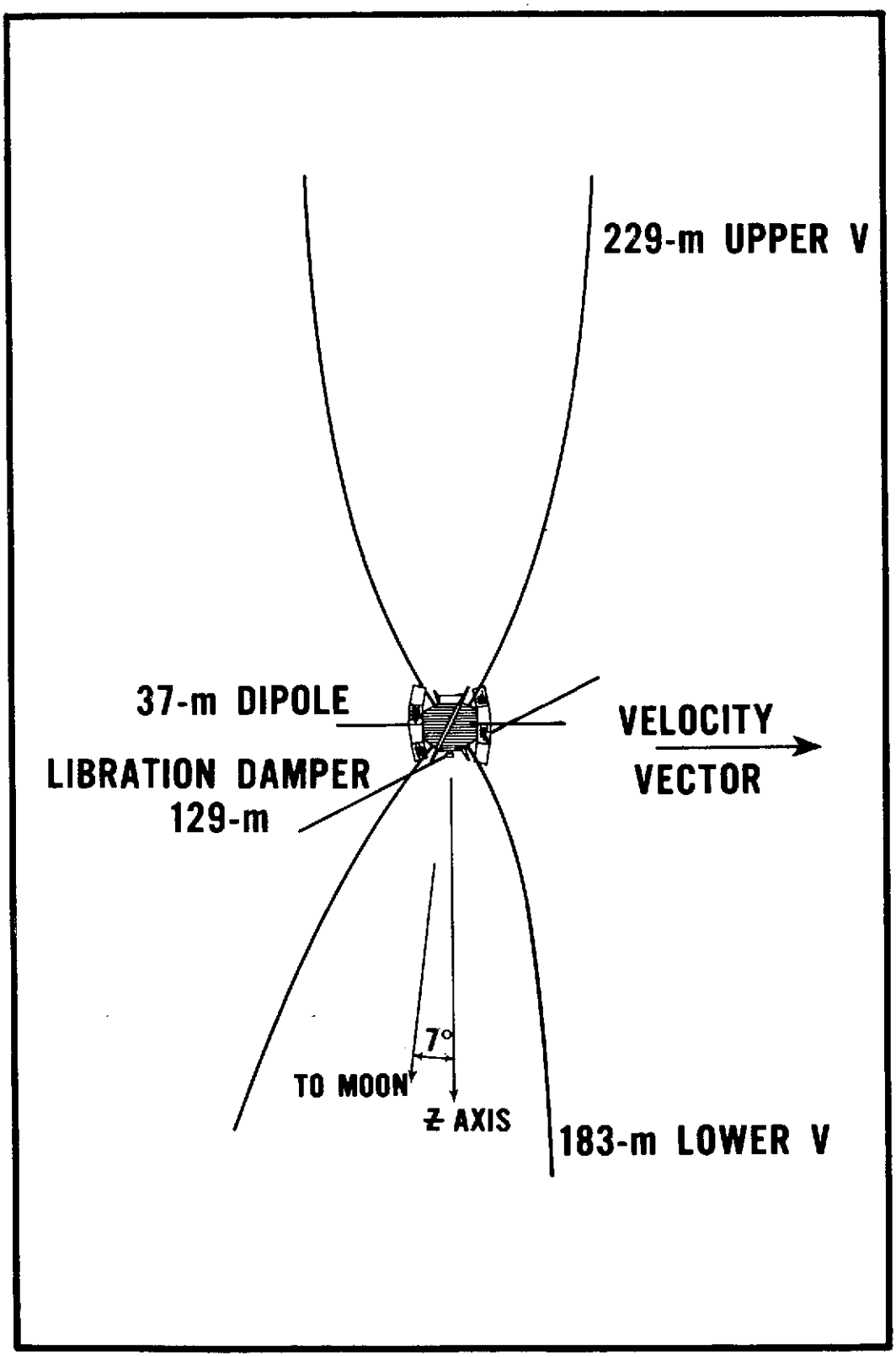
229-m UPPER V
37-m DIPOLE
LIBRATION DAMPER
129-m
VELOCITY
VECTOR
7°
TO MOON
Z AXIS
183-m LOWER V

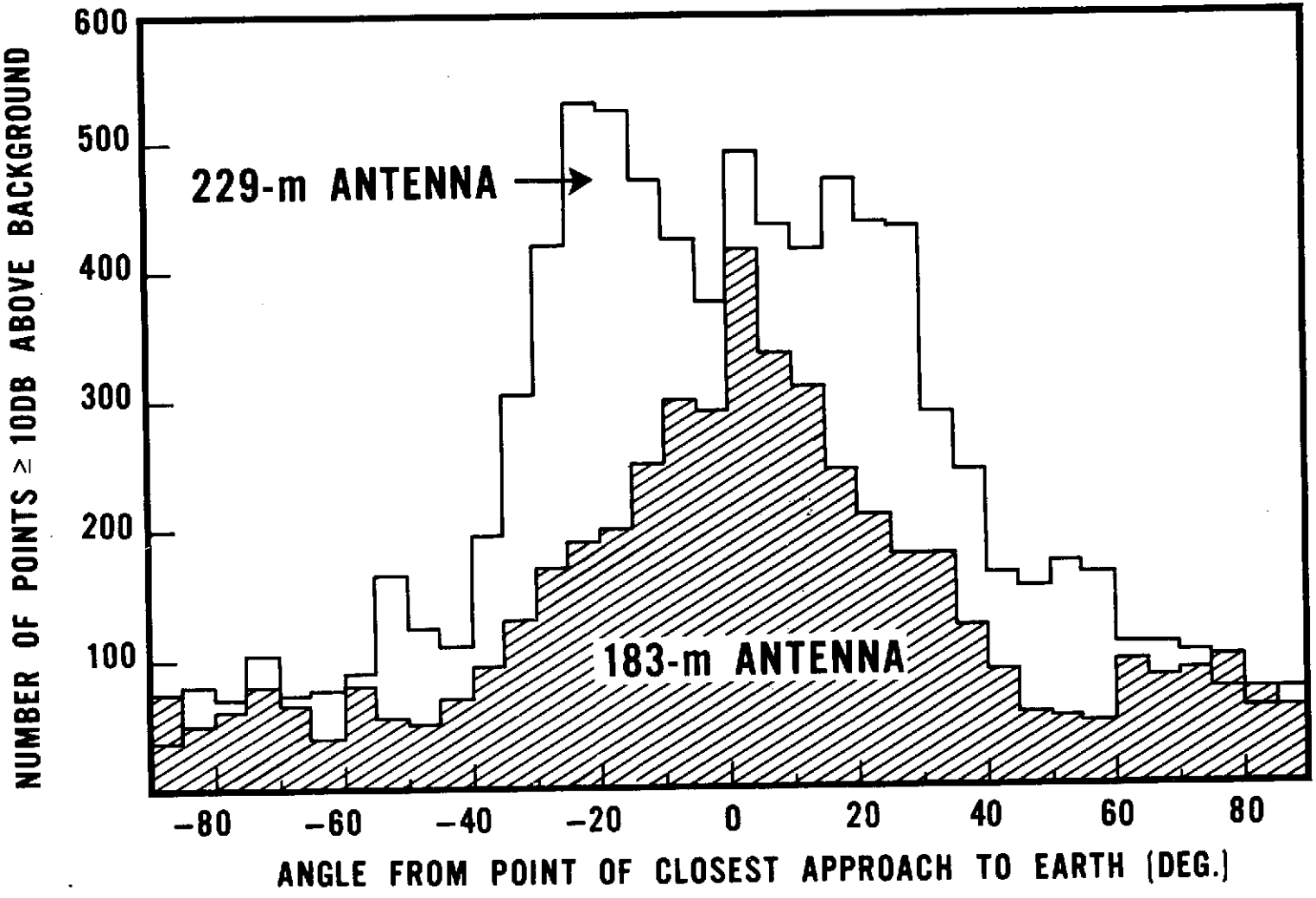
600
500
400
300
200
100
NUMBER OF POINTS ≥ 10DB ABOVE BACKGROUND
229-m ANTENNA
183-m ANTENNA
-80
-60
-40
-20
0
20
40
60
80
ANGLE FROM POINT OF CLOSEST APPROACH TO EARTH (DEG.)

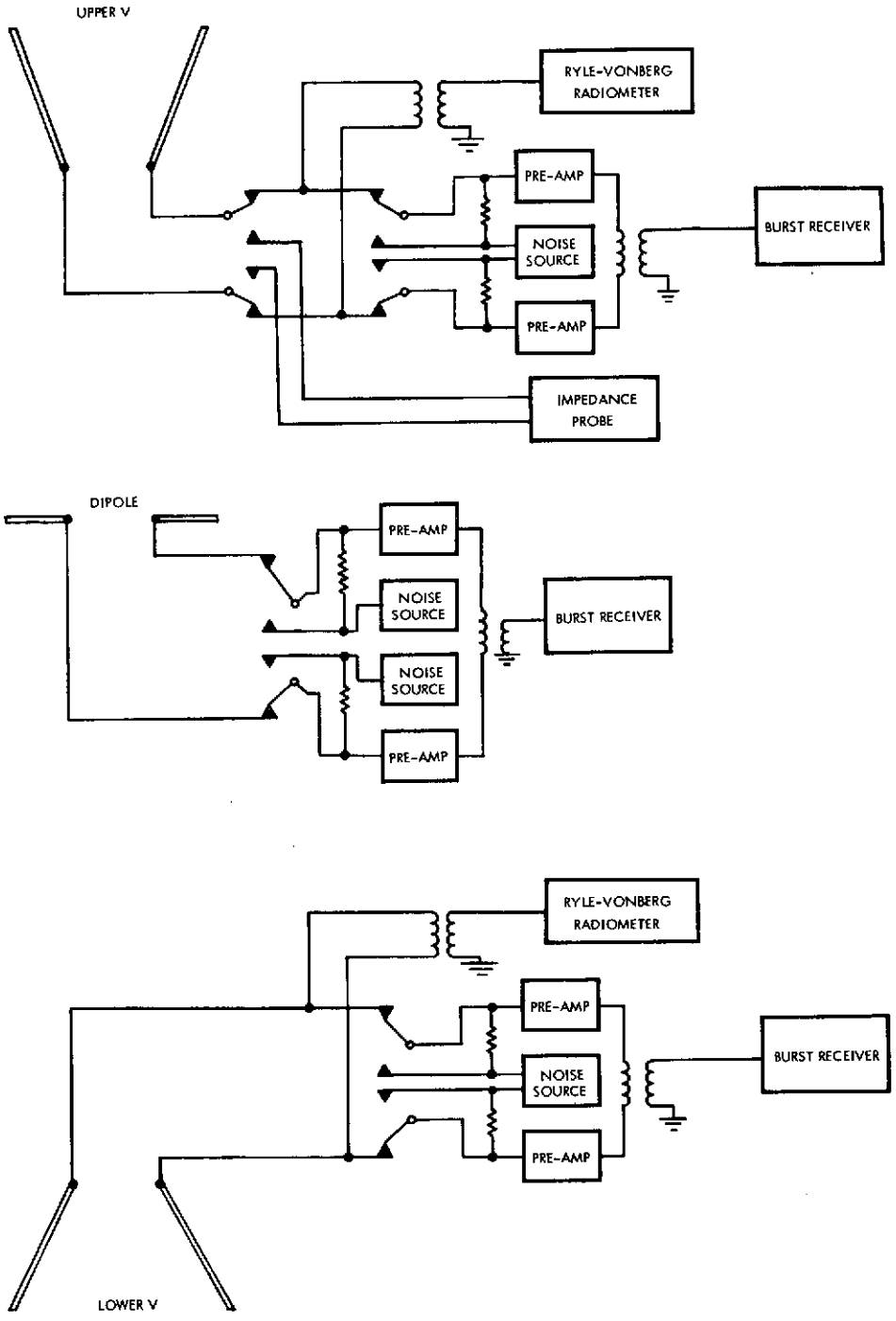

ORIGINAL PAGE IS
OF POOR QUALITY

ORIGINAL PAGE IS
OF POOR QUALITY

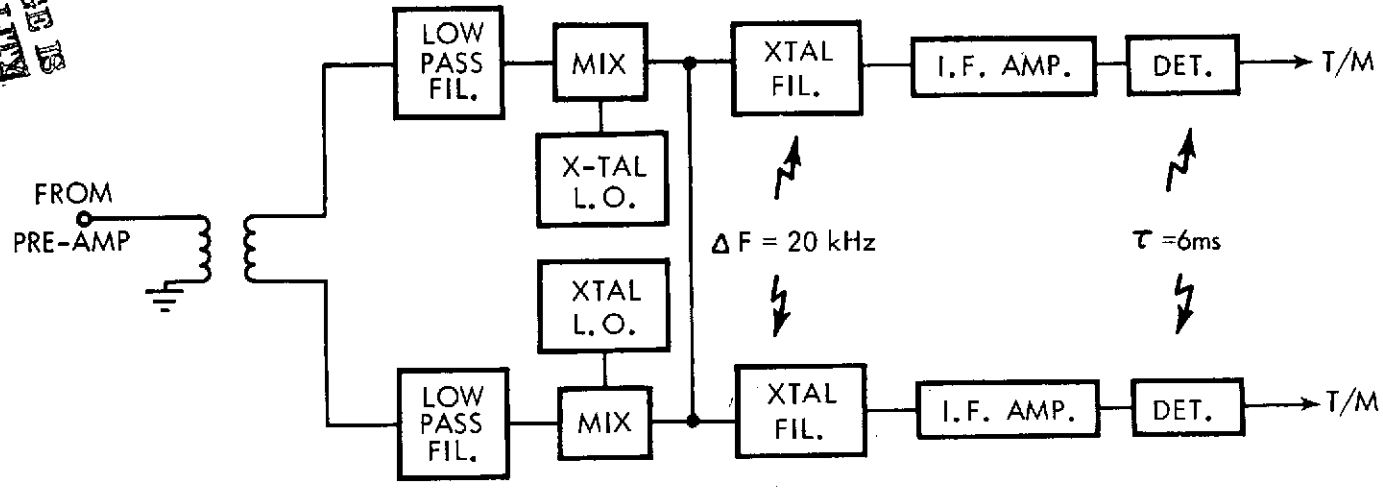

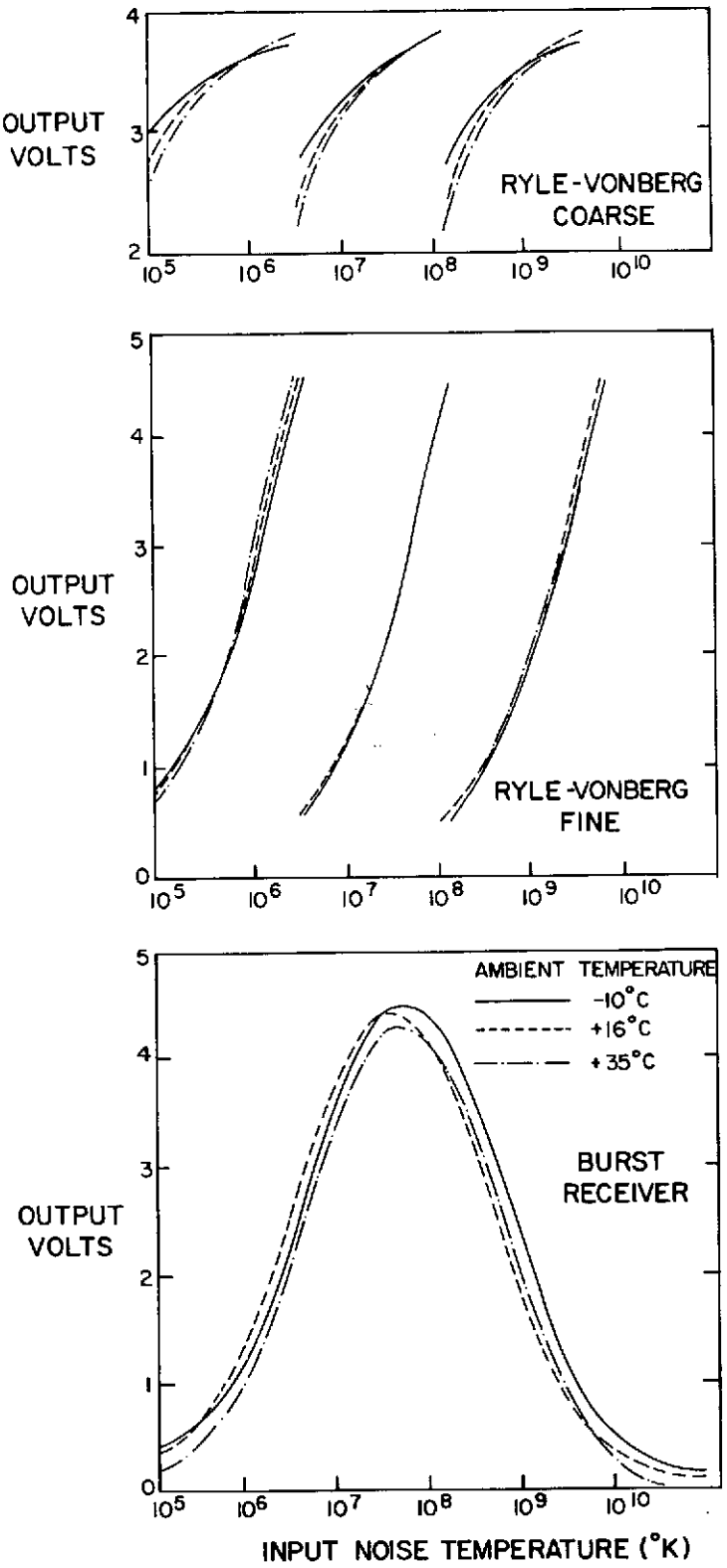
OUTPUT VOLTS
RYLE-VONBERG COARSE
OUTPUT VOLTS
RYLE-VONBERG FINE
OUTPUT VOLTS
AMBIENT TEMPERATURE
-10°C
+16°C
+35°C
BURST RECEIVER
INPUT NOISE TEMPERATURE (°K)

ORIGINAL PAGE IS
OF POOR QUALITY

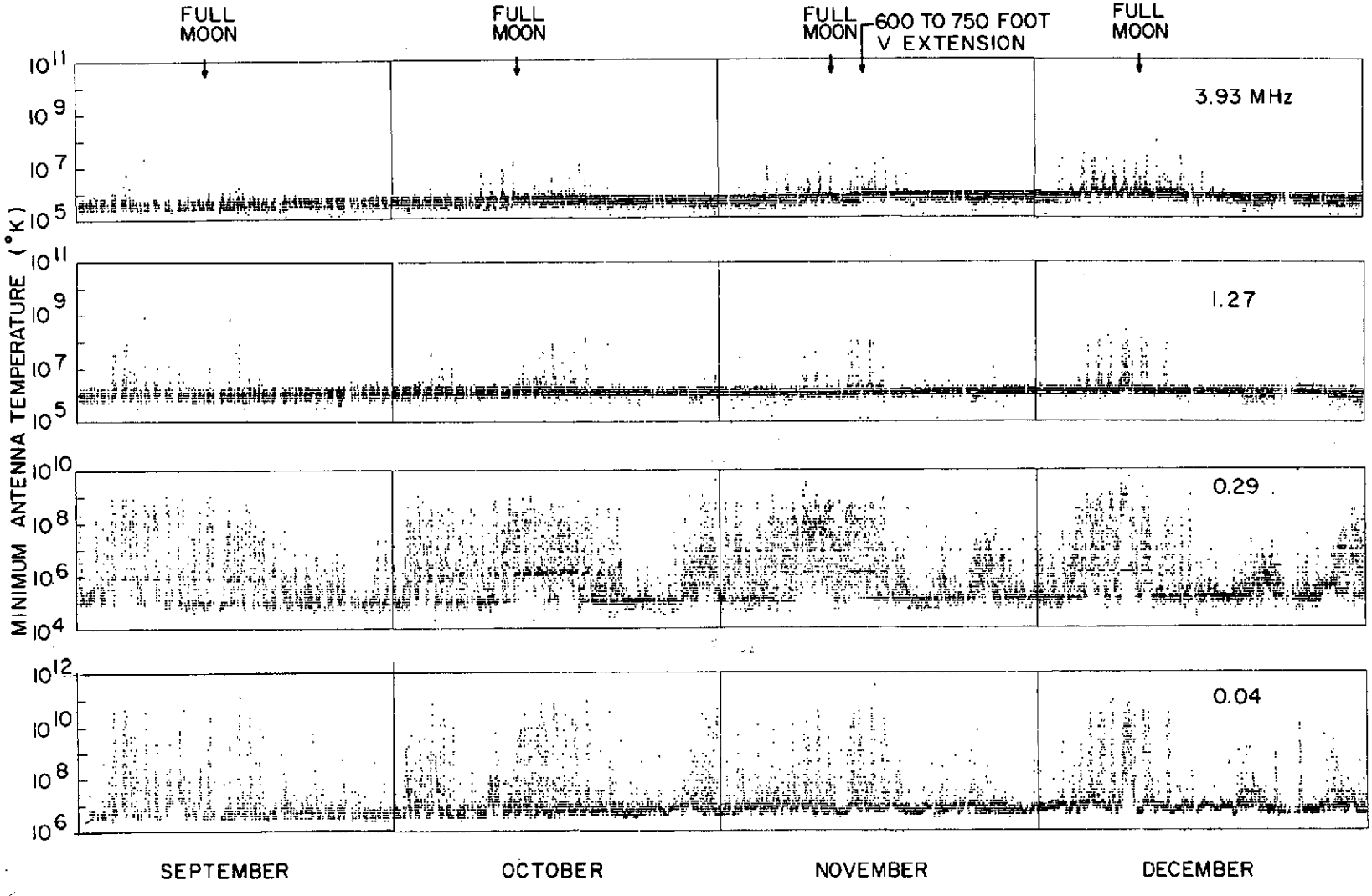

ORIGINAL PAGE IS
OF POOR QUALITY